Bulletin of the Seismological Society of America, Vol. 99, No. 5, pp. 3077–3085, October 2009, doi: 10.1785/0120080361

Short Note

The Puzzle of the 1996 Bárdarbunga, Iceland, Earthquake: No Volumetric Component in the Source Mechanism

by Hrvoje Tkalčić, Douglas S. Dreger, Gillian R. Foulger, and Bruce R. Julian

Abstract A volcanic earthquake with M_w 5.6 occurred beneath the Bárdarbunga caldera in Iceland on 29 September 1996. This earthquake is one of a decade-long sequence of M 5+ events at Bárdarbunga with non-double-couple mechanisms in the Global Centroid Moment Tensor catalog. Fortunately, it was recorded well by the regional-scale Iceland Hotspot Project seismic experiment. We investigated the event with a complete moment tensor inversion method using regional long-period seismic waveforms and a composite structural model. The moment tensor inversion using data from stations of the Iceland Hotspot Project yields a non-double-couple solution with a 67% vertically oriented compensated linear vector dipole component, a 32% double-couple component, and a statistically insignificant (2%) volumetric (isotropic) contraction. This indicates the absence of a net volumetric component, which is puzzling in the case of a large volcanic earthquake that apparently is not explained by shear slip on a planar fault. A possible volcanic mechanism that can produce an earthquake without a volumetric component involves two offset sources with similar but opposite volume changes. We show that although such a model cannot be ruled out, the circumstances under which it could happen are rare.

Introduction

A remarkable series of seismic and magmatic events beneath the Vatnajökull icecap in Iceland occurred in 1996 and ultimately led to a breakout flood (jökulhlaup) from the Grimsvötn volcano subglacial caldera lake. A sequence of earthquakes commenced 29 September starting with a magnitude 5.6 earthquake in the Bárdarbunga volcano (Fig. 1). Similar earthquakes had occurred in this area previously. Ten earthquakes clustered around the Bárdarbunga caldera are reported in the Harvard Centroid Moment Tensor catalog for the period 1976–1996 (Nettles and Ekström, 1998). However, this time the event was followed by a swarm of small earthquakes that migrated toward a neighboring volcano, Grímsvötn, and culminated in a subglacial volcanic eruption (Nettles and Ekström, 1998).

The main event, an M_w 5.6 earthquake, displayed an unusual pattern of seismic radiation, suggesting a non-double-couple (NDC) mechanism. Studies of the event using teleseismic long-period and intermediate period surface-wave data (Nettles and Ekström, 1998) and regional Icelandic data, based on a simple one-dimensional wave-speed model (Konstantinou *et al.*, 2003) gave solutions with large compensated linear vector dipole (CLVD) components with approximately vertical oriented tensional major dipoles. Nettles and Ekström (1998) proposed that the derived NDC source mechanisms result from slip on an outward-dipping cone-shaped ring fault beneath the caldera, as a result of a change in pressure in the volcano's shallow magma chamber. Konstantinou *et al.* (2003) also reported an (8.5%) implosive isotropic component and concluded that it was statistically significant. In this article, we decompose moment tensors using the scheme of Knopoff and Randall (1970), described in section 2.6 of Julian *et al.* (1998).

Previous Studies of Non-Double-Couple Seismic Sources

A double-couple (DC) is a theoretical force system that would generate, in a medium without discontinuity, the same elastic field as a shear dislocation. It is the conventional representation of a shear fault as a point source (e.g., Kostrov and Das, 1989). A pure DC produces a quadrantal distribution of the polarities of elastic compressional waves. The symmetric second-rank seismic moment tensor, M, provides a general representation of an arbitrarily oriented seismic source having in general DC, CLVD, and isotropic components. The physical source processes that produce NDC moment tensors are not well understood, but the effort to interpret them is usually approached by decomposing the

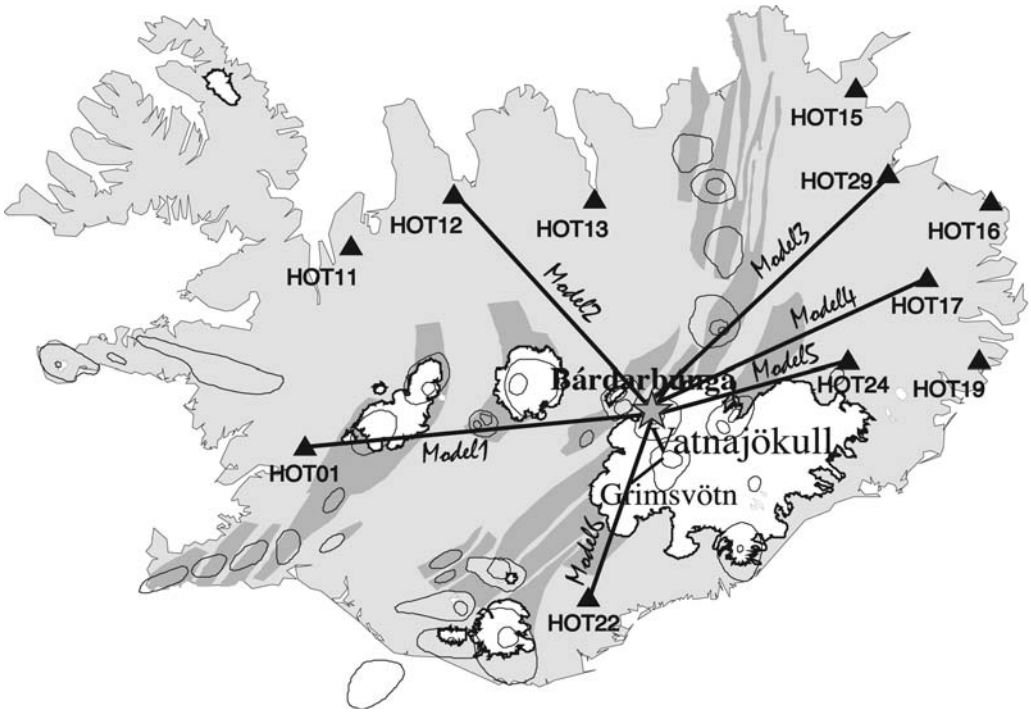

Figure 1. Map showing the main tectonic and volcanic features in Iceland. Glaciers are shown in white and spreading segments in dark gray. Volcanoes are shown with thin lines. The Bárdarbunga earthquake is shown with the gray star. Triangles are locations of the 11 Iceland Hotspot Project broadband stations used in the moment tensor inversion. Lines indicate the locations of the six different one-dimensional models used between the source and stations.

tensor into DC, CLVD, and isotropic components. We follow this approach in the present analysis.

A CLVD corresponds to three orthogonal dipoles with moments in the ratio $2:-1:-1$, so that there is no net change in volume. The dominant dipole can be either compressional or dilatational (with the other dipoles of opposite polarity). A pure CLVD point source has two cylindrical nodal surfaces. The isotropic component measures any volume change in an earthquake. The CLVD component of a tectonic earthquake typically contains less than 30% of the total seismic moment. Unusually, in the case of the Bárdarbunga earthquake, the CLVD component is dominant over the DC component and involves an outward-orientated, vertical major dipole.

NDC earthquakes with CLVD components have been attributed to several physical mechanisms. These include tensile failure (e.g., Julian, 1983; Foulger and Long, 1984; Julian and Sipkin, 1985; Julian *et al.*, 1997; Miller *et al.*, 1998; Foulger *et al.*, 2004), complex faulting, for example, involving multiple ruptures on a transform fault or mid-ocean ridge (Kawakatsu, 1991), and nonplanar rupture (Frolich, 1994; Kuge and Lay, 1994; Julian *et al.*, 1998). In addition, dip-slip shear faulting on a conical fault spanning a large range of strikes theoretically also has an NDC component (Ekström, 1994; Frolich, 1994; Julian *et al.*, 1998). This latter mechanism is a possible candidate for the 29 September 1996 event. We tested it through numerical simulation of the finite rupture process for an outward-dipping ring fault using a three-dimensional finite-difference method and were unable to reject the hypothesis (Tkalčić *et al.*, 2005).

In parallel with understanding physical mechanisms responsible for the presence of NDC components in the moment tensor, several methods have been developed. An efficient method, called INdirect PARameterization, of determining simultaneously moment tensor and source time function in the presence of a high noise-to-signal ratio, was developed by Šilený and Panza (1991) and Šilený *et al.* (1992). The method utilizes the information from complete waveforms synthesized by a modal summation and takes into account the effects of the noise, the mislocation, and the uncertainty in the velocity structure. It has been tested and applied in various settings including volcanic and geothermal (e.g., Panza *et al.*, 1993; Cespuglio *et al.*, 1996; Panza and Sarao, 2000; Guidarelli and Panza, 2006). Another efficient method, which uses linear programming to perform complete moment tensor analysis (including NDC components), was developed by Julian and Foulger (1996). The method utilizes the information from amplitude ratios to circumvent the effects of complex Earth structure on seismic waveforms. It has been applied to earthquakes at several volcanic and geothermal areas with great success (e.g., Julian *et al.*, 1997; Miller *et al.*, 1998; Foulger *et al.*, 2004).

Here, we report the complete seismic moment tensor. We find no evidence in support of a significant isotropic component. Because volcanic earthquakes are frequently accompanied by the movement of magma and other dynamic

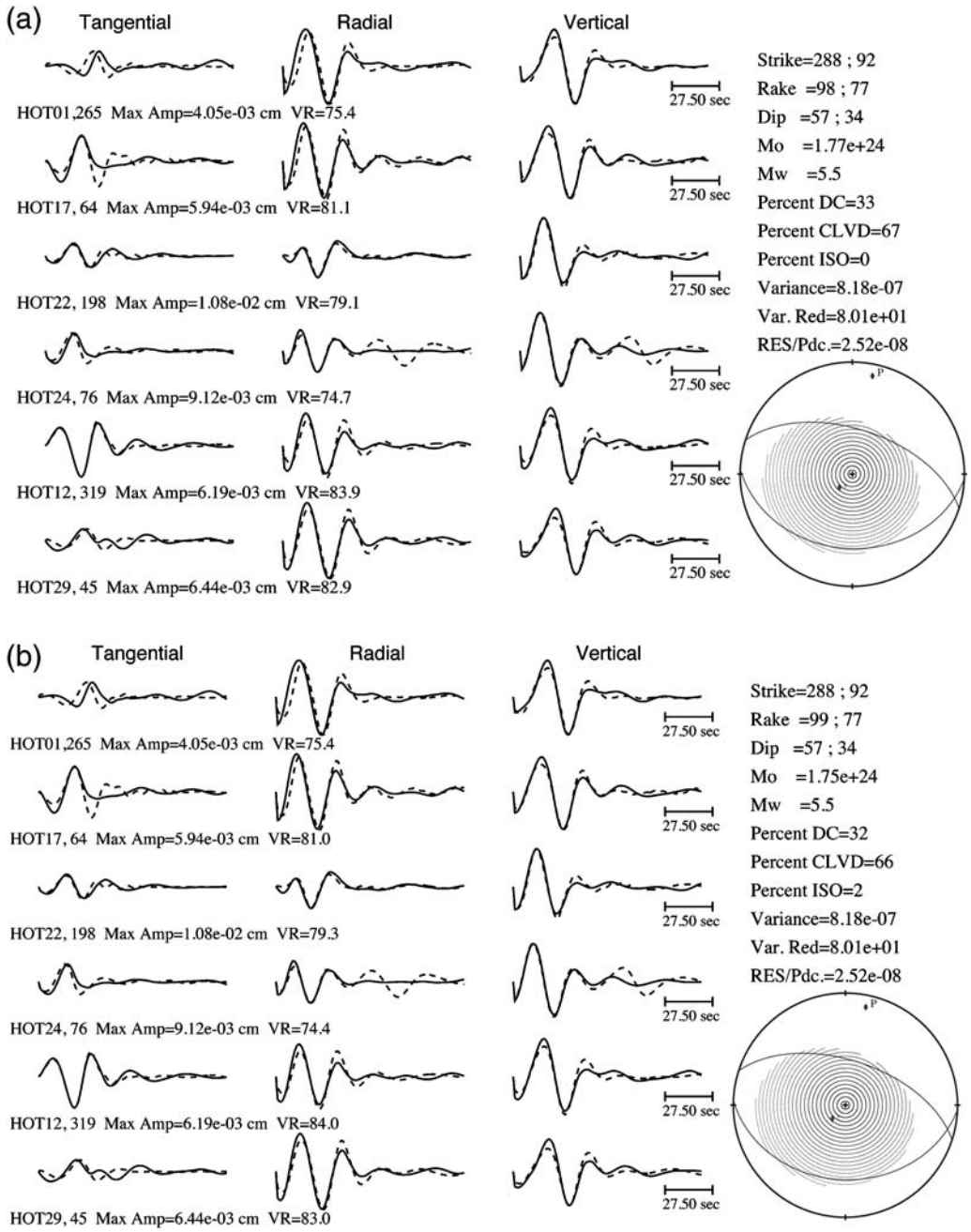

Figure 2. Comparison of (a) deviatoric and (b) full moment tensor point-source inversion results for the Bárdarbunga event. Three-component displacement seismograms (tangential, radial, and vertical, from left to right) are shown by solid lines and compared to one-dimensional synthetic seismograms (dashed lines). The lower-hemisphere projection of the *P*-wave radiation pattern is shown at right. The strike, rake, and dip of the two nodal planes of the best DC solution, as well as the scalar seismic moment, moment magnitude, and percentage DC, CLVD, and isotropic, are given numerically at right.

processes such as opening of cracks induced by pressurized fluids, this result is surprising. We discuss the feasibility of a volcanic model with a mass-exchange mechanism that produces no net volume change.

Seismic Data and Wave-Speed Models for Iceland

A useful dataset with which to study the event was collected by the regional-scale Iceland hotspot seismic experiment (Foulger *et al.*, 2001). Studies using these data have resolved many details of the complex crustal structure of Iceland. For example, Du and Foulger (1999, 2001) and Du *et al.* (2002) used teleseismic receiver functions and surface-wave dispersion measurements to obtain the laterally varying wave-speed structure beneath Iceland. Crustal thickness was determined using a combination of seismic profiles, receiver functions, and gravity profiles (Darbyshire *et al.*, 2000; Foulger *et al.*, 2003). Another study used seismic

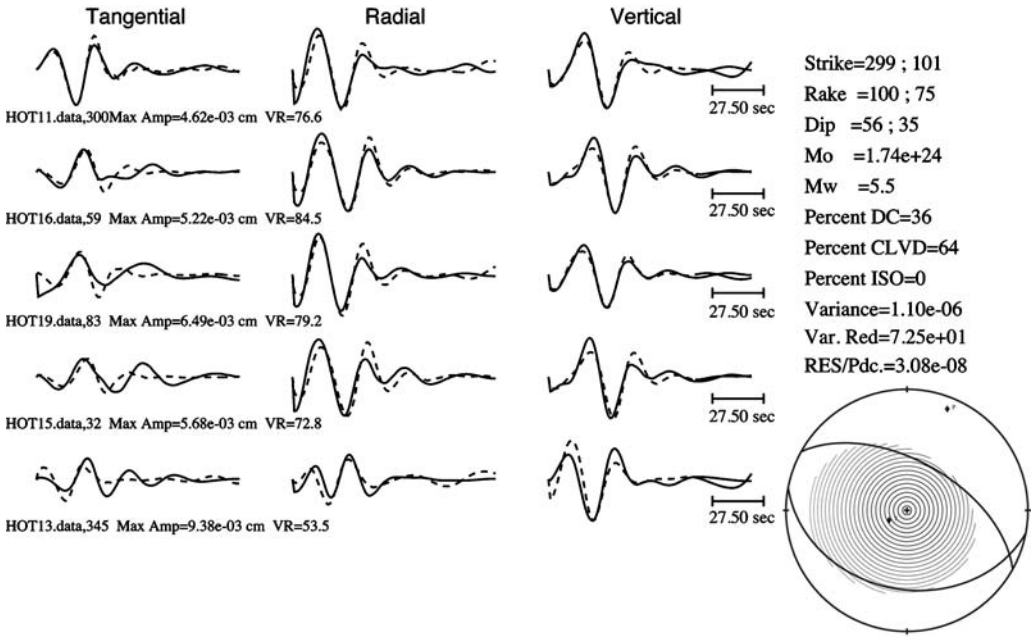

Figure 3. Three component observed and synthetic displacement seismograms for a point-source moment tensor inversion for another, independent set of stations, whose locations are shown in Figure 1. Compare with Figure 2a.

tomography to constrain the structure under Iceland (Foulger *et al.*, 2000, 2001). These studies demonstrate the high degree of complexity of crustal structure beneath Iceland.

In the present study, the most difficult task was determining Green's functions. Utilizing a frequency wavenumber integration (FKI) program (Saikia, 1994), we generated Green's functions for (a) an average *S*-wave crustal tomography model (Allen *et al.*, 2002) and (b) crustal models determined by jointly inverting teleseismic receiver functions and surface-wave dispersion curves (Du and Foulger, 1999). Using a single model for Iceland to compute Green's functions for all source-receiver paths did not yield good fits to the observed waveforms, especially when waveforms from more than two stations were analyzed. We obtained significantly better results when we used the separate wave-speed models of Du and Foulger (1999) to compute Green's functions. This was true despite the fact that teleseismic receiver functions are sensitive only to the structure under a seismometer (with some lateral sensitivity), while Green's functions depend on the structure along the entire source-receiver path.

The Lack of a Volumetric Component in the Moment Tensor

We used the full-waveform inversion method described by Pasyanos *et al.* (1996). We obtained both deviatoric (where M is decomposed into only DC and CLVD components) and full moment tensor (FMT) solutions. The FMT inversion allows for an isotropic component (explosive or implosive volume change). Recovery of a statistically significant component of this kind is strong evidence for direct fluid involvement in the source process (e.g., Dreger *et al.*, 2000).

The method inverts three-component, long-period (0.02–0.05 Hz) seismograms for the six independent elements of the seismic moment tensor. A synchronous and impulsive source time function and a point source are assumed, and depth is determined through an iterative process. Using this method, we previously demonstrated the existence of large volumetric components in earthquakes from the Long Valley caldera, California (Dreger *et al.*, 2000). Several studies have demonstrated that the method is insensitive to lateral and vertical inhomogeneities along ray paths and near-source or near-receiver structure but is sensitive to the source orientation and depth for the passband employed by the inversion method (e.g., Dreger and Helmberger, 1993; Panning *et al.*, 2001).

We examined all the waveform data available from Iceland Hotspot Project stations. For the bulk of the analysis we used six stations with excellent azimuthal coverage: HOT01, HOT12, HOT17, HOT22, HOT24, and HOT29 (Fig. 1). The deviatoric inversion of data from these stations yielded an NDC solution with a 67% CLVD component (Fig. 2a), while the FMT resulted in a similar 66% CLVD component accompanied by an insignificant volumetric contraction (isotropic component = 2%; Fig. 2b). Inversions using data from other groups of stations confirmed that the result is stable and well constrained. One such configuration of stations with the corresponding best fits and the results of deviatoric inversion is shown in Figure 3 (both deviatoric and FMT inversions were performed). Again, the volumetric part was insignificant, and there was no improvement in variance reduction when volumetric component was

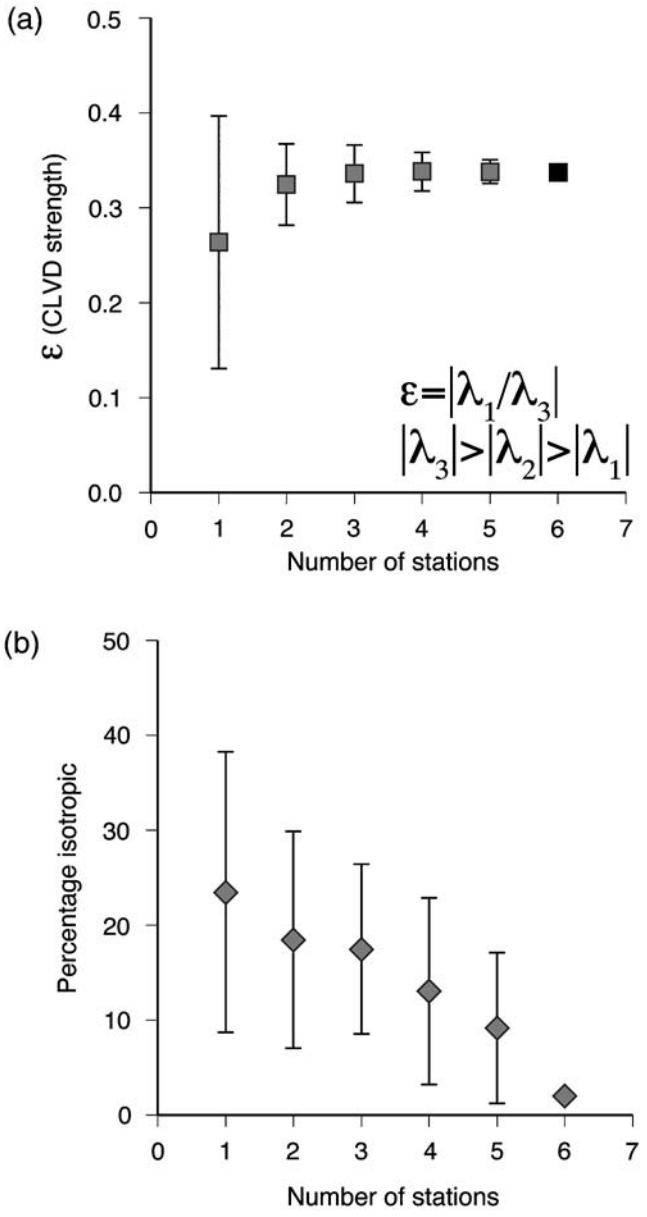

Figure 4. Jackknife sensitivity test, illustrating the stability of (a) the CLVD, presented by the value of ε, where ε is a measure of the size of the CLVD component relative to the DC, and λ_i are the deviatoric eigenvalues of M; (b) the isotropic components, as a function of the number of stations used in the inversion. The symbols show the mean percent isotropic component ± 1 standard deviation error bars.

allowed in the moment tensor. This consistency of solutions for different configurations of stations demonstrates the robustness of the moment tensor solution. This is a consequence of the excellent azimuthal coverage and good structural models. From the calculated 5 min waveforms, we used 110 sec when inverting for moment tensors.

The depth estimate of Nettles and Ekström (1998) of 3.5 km is based on a broadband analysis for depth and duration of moment release. For high frequencies, we estimated the nucleation depth of the event to be 3.9 km from first-arrival-time analysis. At low frequencies, in the moment tensor inversion, we tested 1.5, 3.5, and 5.5 km depths and obtained the best results for 3.5 km depth. The depth estimates obtained using different frequency bands generally agree well.

We performed a sensitivity test to examine the stability of the CLVD component expressed as the value of ε, a measure of the size of the CLVD component (e.g., Dziewonski *et al.*, 1981; Julian *et al.*, 1998, equation 18; Figure 4a) and the isotropic component (Fig. 4b) to the number of stations used in the inversion. We found that six stations can adequately resolve any possible isotropic component. As can be seen from Figure 4, after the number of the waveforms reaches three, the strength of the CLVD component ceases to vary as new waveforms are added, reaching a value of about 0.35. The overall variance reduction does not decrease significantly with the addition of stations. While for a single station the variance reduction can reach 90%, this number drops to about 85% for three to four stations and is slightly over 80% for six stations. On the other hand, the isotropic component decreases with increasing number of waveforms used in the inversion.

Clearly, one station is insufficient to estimate the strength of the CLVD component, and even three stations still yield relatively strong (and erroneous) isotropic components. Certain combinations of four stations also give erroneous results. For example, when HOT01 and HOT22 are excluded from the inversion, azimuthal coverage becomes extremely poor and the result is a strong horizontal CLVD (Fig. 5). Despite the fact that it was shown previously that it is possible to detect explosive earthquake components with as few as three stations (Dreger and Woods, 2002), the results shown here illustrate the importance of good azimuthal coverage. A similar result was obtained by Šilený *et al.* (1996), who pointed out the important roles of azimuthal coverage and minimum number of stations in the moment tensor inversion. Our results also indicate the sensitivity of the moment tensor inversion to the quality of the Green's functions, which supports earlier findings of Cespuglio *et al.* (1996) about possible contamination of the retrieved source mechanism by inaccurate knowledge of the relevant structural models.

We conducted an additional numerical search for pure DC moment tensors and also ones with DC and isotropic components, but we obtained significantly poorer fits to the data. We also investigated the potential biases that could have been introduced by net forces in the physical process. Some workers have handled this problem by including three net-force components in the source representation (e.g., Chouet *et al.*, 2003). The existence of a net force, however, cannot hinder recovery of an isotropic component in our inversion. The inversion is linear with an isotropic component allowed, so if there is one, it would have been retrieved.

Volume (Mass) Exchange Mechanism

NDC earthquakes with vertically oriented CLVD components occur at Bárdarbunga repeatedly (see, e.g., Fig. 1 of

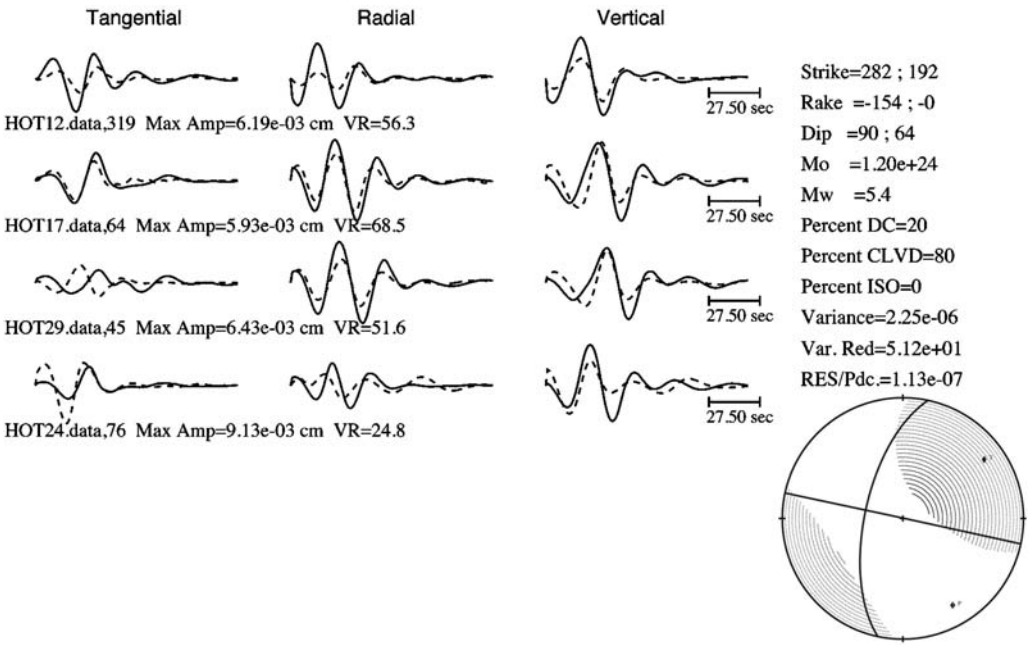

Figure 5. The inversion results for a point-source moment tensor inversion for the case of poor azimuthal coverage. HOT01 and HOT22 are excluded from the inversion, and this results in a strong horizontal CLVD. Compare with Figures 2a and 3.

Nettles and Ekström, 1998). Although we are able to model the observed focal mechanism using slip on a ring fault (Tkalčić *et al.*, 2005), in practice, outward-dipping ring dikes are usually near-vertical, and therefore, not efficient generators of non-double-couple mechanisms. Cone sheets have smaller dip angles and would be more efficient, but they dip inward. It is not well understood under which circumstances, and if at all, ring dikes or cone sheets can rejuvenate to form faults. This argues for exploring an alternative, a nontectonic source, to explain the lack of volumetric components in the moment tensor for this earthquake. In addition, there are indications from smaller aftershocks whose mechanisms we analyzed using the method of Julian (1986) and Julian and Foulger (1996) that in at least two cases (for smaller aftershocks) the focal mechanisms are similar to that for the main event. It is hard to reproduce this kind of scaling in focal mechanisms with earthquakes generated by a slip on a nonplanar fault because proportionally a smaller portion of the circumference rupturing will not yield the vertical CLVD component.

We, therefore, considered a mass-exchange process that can yield a NDC mechanism and still produce a negligible volumetric component. This could be two magma chambers, a deeper and a shallower one, with exchange of magma or pressurized liquid between them (Fig. 6a) or a magma chamber and an opening crack (Fig. 6b). The major difference between this mechanism and that proposed by Nettles and Ekström (1998) is that the NDC radiation by magma movement eliminates the need for fault segments slipping, and at the same time, explains the lack of volumetric components in the moment tensor. This is an attractive hypothesis because it would be also possible to reproduce the observed vertical

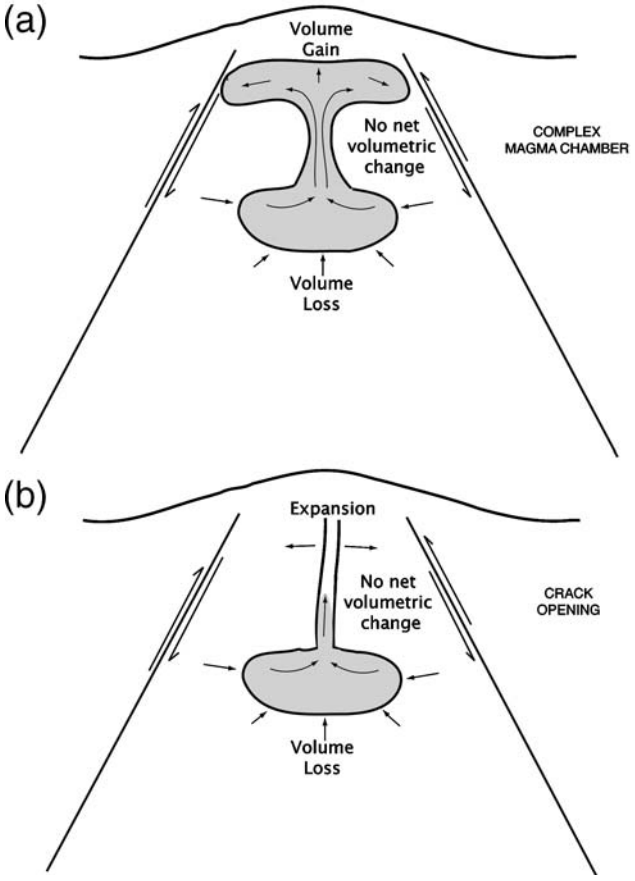

Figure 6. Sketch of tested models with two compensating sources reproducing a vertically oriented CLVD in dilatation (where volumetric exchange is equal and opposite in sign): (a) a complex magma chamber and (b) an implosive source and a vertical, horizontally opening crack above.

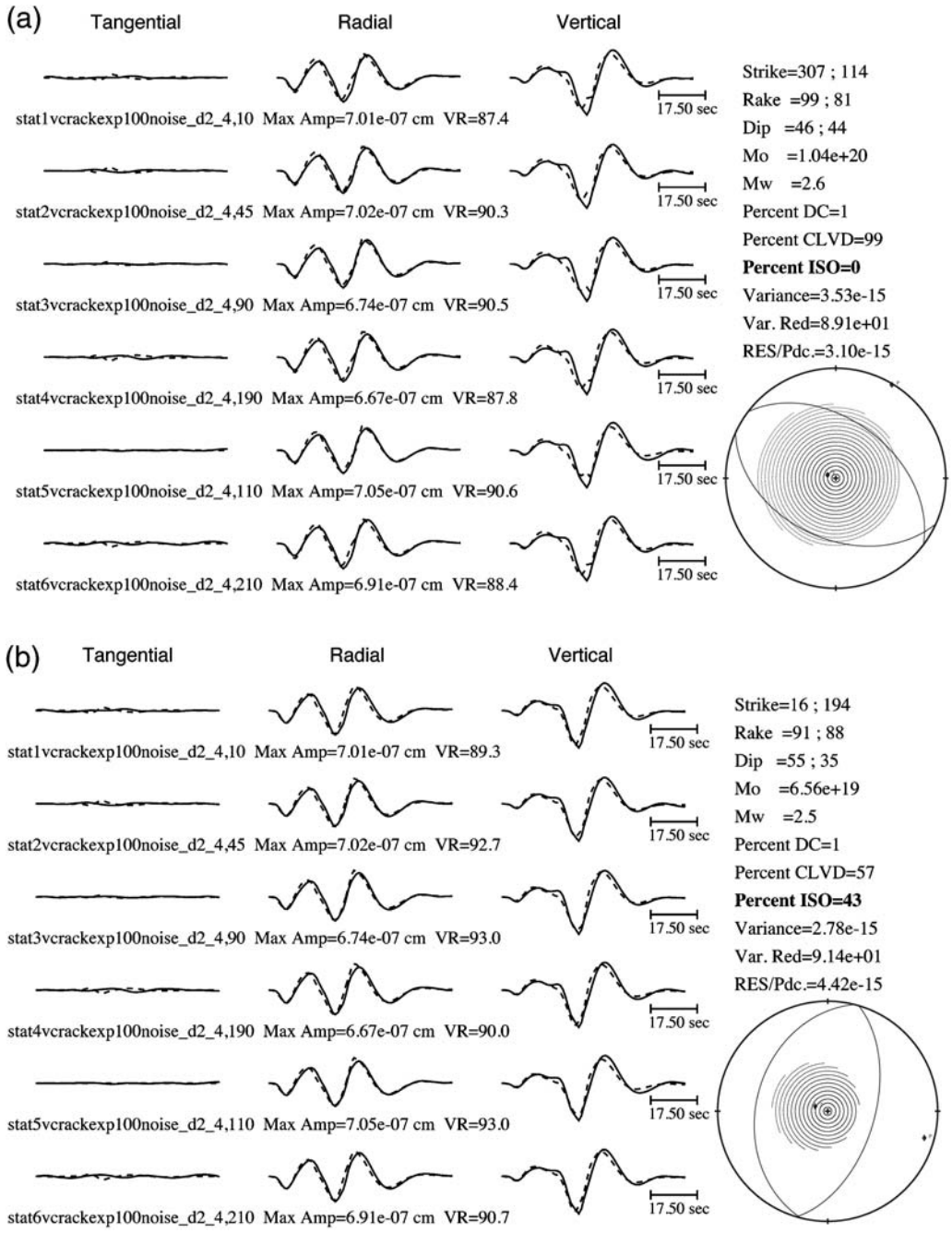

Figure 7. As Figure 2 but showing (a) deviatoric and (b) full moment tensor inversions using a model of two fully compensating sources, an implosive source 4 km deep, and a horizontally opening crack 2 km deep. The waveforms corresponding to these sources are shown by solid lines and are used as synthetic data. 10% noise is included. The modeled waveforms are one-dimensional Green's functions based on slightly imperfect wave-speed models (dashed lines) and a depth of 3 km. Statistically significant improvement in waveform fits is obtained and a large volumetric component is retrieved for a full moment tensor inversion.

CLVD by different configurations and depths of inflating and deflating pairs of magma chambers or a single magma chamber and an opening crack. It would be possible for this mechanism to be accompanied by tectonic events with reverse focal mechanisms in the case of a shallow magma chamber pushing on the inner side of the caldera walls downwards.

Using the regional moment tensor inversion method (see previous section), we performed a synthetic data grid search analysis of models with various levels of volume compensation (the explosive component of the first source being compensated by the implosive component of the second) and distances between the two sources. Such volume compensation is required to explain the lack of statistically significant volumetric component in the observed waveforms. The grid search results showed that, given a reasonable uncertainty in source depth and using imperfect Green's functions with

noise, a vertically offset horizontal crack and deeper volumetric source could result in a large observed isotropic component even with the long-period waveforms used. Also, it is likely that this large isotropic component would be statistically significant, which is inconsistent with the observations for the Bárdarbunga earthquake. For two completely mutually compensating sources (i.e., when the explosive component of the first source equals the implosive component of the second), a grid search using 1 km steps in source depth and with the vertical distance between the two sources less than or equal to 3 km, yields 69 cases. In 59 of these cases, the isotropic component obtained is more than 10% of the total moment. In 41 of the cases, an isotropic component is resolved and is statistically significant at the 90% level or higher.

Figure 7 shows examples of the deviatoric (Fig. 7a) and full moment tensor (Fig. 7b) inversion results for two mutually compensating sources: an implosion at 4 km depth and a horizontal, vertically opening crack at 2 km depth. This corresponds most closely to the diagram shown in Figure 6a and produces a mechanism such as that of the Bárdarbunga event. The waveforms corresponding to this configuration of sources are shown by solid lines. 10% of random noise was introduced, which is comparable to the noise level for the Bárdarbunga earthquake data. Synthetic waveforms are one-dimensional Green's functions, based on slightly imperfect wave-speed models (shown by dashed lines) and a depth of 3 km. As Figure 7b shows, statistically significant improvement in waveform fits and large, yet false isotropic component is retrieved from the inversion. This is opposite from what was observed for the 1996 Bárdarbunga earthquake.

Conclusions

We used regional seismic waveforms and a detailed structural model to invert for the full moment tensor of the 1996 Bárdarbunga earthquake. The deviatoric inversion yields a non-double-couple solution, in which the moment tensor is dominated by a vertically oriented compensated linear vector dipole component (67%). The full moment tensor solution shows a similar, 66% compensated linear vector dipole component, 32% double-couple component, and a statistically insignificant 2% volumetric (isotropic) contraction, indicating the lack of net volumetric component. This is a puzzling result from a volcanic environment. A possible volcanic mechanism that produces such an earthquake involves two offset sources with similar but opposite volume changes. We show that although such a model cannot be ruled out, it is unlikely.

Data and Resources

Seismograms and station information are available from the Incorporated Research Institutions for Seismology Data Management Center at www.iris.edu (last accessed June 2009). Figures were made with the General Mapping Tools (www.soest.hawaii.edu/gmt [last accessed July 2009]; Wessel and Smith, 1995). Synthetic seismograms are computed using a wave-number integration program by S. Saikia. Together with other software used in this study, it is listed in the references.

Acknowledgments

We are grateful the Lawrence Livermore National Laboratory postdoctoral program for supporting H. Tkalčić's time on this project, while he was a postdoctoral research fellow at that institution. We would also like to thank two anonymous reviewers and the Associate Editor Charlotte Rowe, whose comments helped to improve this manuscript.

References

Allen, R. M., G. Nolet, W. J. Morgan, K. Vogfjörd, M. Nettles, G. Ekström, B. H. Bergsson, P. Erlendsson, G. R. Foulger, S. Jakobsdóttir, B. R. Julian, M. Pritchard, S. Ragnarsson, and R. Stefánsson (2002). Plume driven plumbing and crustal formation in Iceland, *J. Geophys. Res.* **107,** doi 10.1029/2001JB000584.

Cespuglio, G., P. Campus, and J. Šilený (1996). Seismic moment tensor resolution by waveform inversion of a few local noisy records—II. Application to the Phlegrean fields (southern Italy) volcanic tremors, *Geophys. J. Int.* **126,** 620–634

Chouet, B., P. Dawson, T. Ohminato, M. Martini, G. Saccorotti, F. Giudicepietro, G. De Luca, G. Milana, and R. Scarpa (2003). Source mechanisms of explosions at Stromboli volcano, Italy, determined from moment tensor inversions of very-long-period data, *J. Geophys. Res.* **108,** 2019, doi 10.1029/2002B001919.

Darbyshire, F. A., R. S. White, and K. F. Priestley (2000). Structure of the crust and uppermost mantle of Iceland from combined seismic and gravity study, *Earth Planet. Sci. Lett.* **181,** 409–428.

Dreger, D. S., and D. V. Helmberger (1993). Determination of source parameters at regional distances with single station or sparse network data, *J. Geophys. Res.* **98,** 8107–8125.

Dreger, D. S., and B. Woods (2002). Regional distance seismic moment tensors of nuclear explosions, *Tectonophysics* **356,** 139–156.

Dreger, D. S., H. Tkalčić, and M. Johnston (2000). Dilational processes accompanying earthquakes in the Long Valley caldera, *Science* **288,** 122–125.

Du, Z. J., and G. R. Foulger (1999). The crustal structure of northwest Iceland from receiver functions and surface waves, *Geophys. J. Int.* **139,** 419–432.

Du, Z. J., and G. R. Foulger (2001). Variation in the crustal structure across central Iceland, *Geophys. J. Int.* **145,** 246–264.

Du, Z. J., G. R. Foulger, B. R. Julian, R. M. Allen, G. Nolet, W. J. Morgan, B. H. Bergsson, P. Erlendsson, S. Jakobsdottir, S. Ragnarsson, R. Stefansson, and K. Vogfjörd (2002). Crustal structure beneath western and eastern Iceland from surface waves and receiver functions, *Geophys. J. Int.* **149,** 349–363.

Dziewonski, A. M., T.-A. Chou, and J. H. Woodhouse (1981). Determination of earthquake source parameters from waveform data for studies of global and regional seismicity, *J. Geophys. Res.* **86,** 2825–2852.

Ekström, G. (1994). Anomalous earthquakes on volcano ring-fault structures, *Earth Planet. Sci. Lett.* **128,** 707–712.

Foulger, G. R., and R. E. Long (1984). Anomalous focal mechanisms: Tensile crack formation on an accreting plate boundary, *Nature* **310,** 43–45.

Foulger, G. R., Z. J. Du, and B. R. Julian (2003). Icelandic-type crust, *Geophys. J. Int.* **155,** 567–590.

Foulger, G. R., B. R. Julian, D. P. Hill, A. M. Pitt, P. Malin, and E. Shalev (2004). Non-double-couple microearthquakes at Long Valley caldera,

California, provide evidence for hydraulic fracturing, *J. Volc. Geotherm. Res.* **132,** 45–71.

Foulger, G. R., M. J. Pritchard, B. R. Julian, J. R. Evans, R. M. Allen, G. Nolet, W. J. Morgan, B. H. Bergsson, P. Erlendsson, S. Jakobsdottir, S. Ragnarsson, R. Stefansson, and K. Vogfjörd (2000). The seismic anomaly beneath Iceland extends down to the mantle transition zone and no deeper, *Geophys. J. Int.* **142,** F1–F5.

Foulger, G. R., M. J. Pritchard, B. R. Julian, J. R. Evans, R. M. Allen, G. Nolet, W. J. Morgan, B. H. Bergsson, P. Erlendsson, S. Jakobsdottir, S. Ragnarsson, R. Stefansson, and K. Vogfjörd (2001). Seismic tomography shows that upwelling beneath Iceland is confined to the upper mantle, *Geophys. J. Int.* **146,** 504–530.

Frohlich, C. (1994). Earthquakes with non-double-couple mechanisms, *Science* **264,** 804–809.

Guidarelli, M., and G. F. Panza (2006). Determination of the seismic moment tensor for local events in the South Shetland Islands and Bransfield Strait, *Geophys. J. Int.* **167,** 684–692.

Julian, B. R. (1983). Evidence for dyke intrusion earthquake mechanisms near Long Valley caldera, California, *Nature* **303,** 323–325.

Julian, B. R. (1986). Analysing seismic-source mechanisms by linear programming methods, *Geophys. J. R. Astr. Soc.* **84,** 431–443.

Julian, B. R., and G. R. Foulger (1996). Earthquake mechanisms from linear-programming inversion of seismic-wave amplitude ratios, *Bull. Seismol. Soc. Am.* **86,** 972–980.

Julian, B. R., and S. A. Sipkin (1985). Earthquake processes in the Long Valley caldera area, California, *J. Geophys. Res.* **90,** 11,155–11,169.

Julian, B. R., A. D. Miller, and G. R. Foulger (1997). Non-double-couple earthquake mechanisms at the Hengill-Grensdalur volcanic complex, southwest Iceland, *Geophys. Res. Lett.* **24,** 743–746.

Julian, B. R., A. D. Miller, and G. R. Foulger (1998). Non-double-couple earthquakes: 1. Theory, *Rev. Geophys.* **36,** 525–550.

Kawakatsu, H. (1991). Enigma of earthquakes at ridge-transform fault plate boundaries: Distribution of non-double couple parameter of Harvard CMT solutions, *Geophys. Res. Lett.* **18,** 1103–1106.

Knopoff, L., and M. J. Randall (1970). The compensated linear vector dipole: A possible mechanism for deep earthquakes, *J. Geophys. Res.* **75,** 4957–4963.

Konstantinou, I. K., H. Kao, C.-H. Lin, and W.-T. Liang (2003). Analysis of broad-band regional waveforms of the 1996 September 29 earthquake at Bárdarbunga volcano, central Iceland: Investigation of the magma injection hypothesis, *Geophys. J. Int.* **154,** 134–145.

Kostrov, B., and S. Das (1989). *Principles of Earthquake Source Mechanics*, Cambridge University Press, Cambridge, United Kingdom.

Kuge, K., and T. Lay (1994). Systematic non-double-couple components of earthquake mechanisms: The role of fault zone irregularity, *J. Geophys Res.* **99,** 15,457–15,467.

Miller, A. D., B. R. Julian, and G. R. Foulger (1998). Three-dimensional seismic structure and moment tensors of non-double-couple earthquakes at the Hengill-Grensdalur volcanic complex, Iceland, *Geophys. J. Int.* **133,** 309–325.

Nettles, M., and G. Ekström (1998). Faulting mechanism of anomalous earthquakes near Bárdarbunga volcano, Iceland, *J. Geophys. Res.* **103,** 17,973–17,983.

Panning, M., D. S. Dreger, and H. Tkalčić (2001). Near-source structure and isotropic moment tensors: A case study of the Long Valley caldera, *Geophys. Res. Lett.* **28,** 1815–1818.

Panza, G. F., and A. Sarao (2000). Monitoring volcanic and geothermal areas by full seismic moment tensor inversion: Are non-double-couple components always artifacts of modeling? *Geophys. J. Int.* **143,** 353–364.

Panza, G. F., J. Šilený, P. Campus, R. Nicolich, and G. Ranieri (1993). Point source moment tensor retrieval in volcanic, geothermal and orogenic areas by complete waveform inversion, *Int. J. Appl. Geophys.* **30,** 98–118

Pasyanos, M. E., D. S. Dreger, and B. Romanowicz (1996). Towards real-time determination of regional moment tensor, *Bull. Seismol. Soc. Am.* **86,** 1255–1269.

Saikia, C. K. (1994). Modified frequency-wavenumber algorithm for regional seismograms using Filon's quadrature; modeling of L_g waves in eastern North America, *Geophys. J. Int.* **118,** 142–158.

Šilený, J., and G. F. Panza (1991). Inversion of seismograms to determine simultaneously the moment tensor components and source time function for a point source buried in a horizontally layered medium, *Studia Geophysica et Geodaetica* **35,** 166–183.

Šilený, J., P. Campus, and G. F. Panza (1996). Seismic moment tensor resolution by waveform inversion of few local noisy records—I. Synthetic tests, *Geophys. J. Int.* **126,** 605–619.

Šilený, J., G. F. Panza, and P. Campus (1992). Waveform inversion for point source moment tensor retrieval with variable hypocentral depth and structural model, *Geophys. J. Int.* **109,** 259–274.

Tkalcic, H., D. S. Dreger, G. R. Foulger, and B. R. Julian (2005). Kinematic modeling and complete moment tensor analysis of the anomalous, vertical CLVD Bardarbunga, Iceland, event, *IASPEI General Assembly*, Santiago de Chile, Chile.

Wessel, P., and W. H. F. Smith (1995). New version of the Generic Mapping Tools released, *Eos Trans. Am. Geophys. Union* **76,** 329.

Research School of Earth Sciences
The Australian National University
Mills Road, Bldg. 61
Canberra 0200 ACT, Australia
Hrvoje.Tkalcic@anu.edu.au
(H.T.)

Berkeley Seismological Laboratory
University of California
Berkeley, California 94720
United States of America
dreger@seismo.berkeley.edu
(D.S.D.)

Department of Earth Sciences
Durham University
Durham DH13LE, United Kingdom
g.r.foulger@durham.ac.uk
(G.R.F.)

United States Geological Survey
Menlo Park, California 94025
United States of America
julian@usgs.gov
(B.R.J.)

Manuscript received 5 December 2008